International journal of imaging science and engineering

ISSN: 1934--9955 www.ijise.net

Vol-15 Issue-01 Aug 2020

Evaluation and Planning of the Base Station for the Satellite Subsystem

Farhan Sultan,

Pakistan

Abstract: This era of fast scientific and technological advancement has made it the standard to improve existing systems on a regular basis. Spending on R&D and keeping up with developments are given top priority. By virtue of its reduced weight and increased stiffness, aluminum has proven to be an effective performance booster in space technology. A satellite support system made of aluminum is the primary object of this study. Designing a support system that meets the stated geometry and stiffness criteria while minimizing bulk is the major aim. A great deal of research went into settling on the final layout. Free vibration analysis was carried out to assess the subsystem's engagement with the underlying structure. We experimented with the structure's design characteristics to do sensitivity analyses. The structure's response to static loads was examined using linear static analysis. Through the use of buckling analysis, the support structure's critical loads were evaluated. The design analysis is carried out using the I-DEAS application, which stands for Design and Analysis.

Keywords: Specifics of the component, evaluation, finite element model, buckling, and statics

1. Introduction

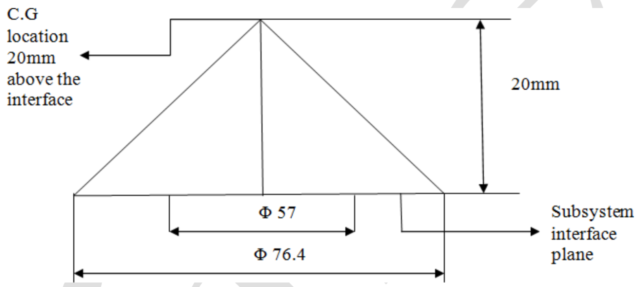

A growing number of factors, including improved payload accuracy and spacecraft structural dynamic behavior while in orbit, are impacting spacecraft design and performance. The current focus is on the assembly design for the support structure of a satellite subsystem with the goal of reducing bulk while maintaining safe operating conditions. Spacecraft forces are crucial for delicate instrumentation. A secure setup that achieves substantial bulk reduction is proposed in this study. To find the best possible setup for the design, we ran sensitivity and normal mode analyses. Such a support system has to be very strong, lightweight, and rigid. The structure has subsystems attached to it and is linked to the satellite's deck. The bracket's upper side is fastened to the satellite's deck.

Lightweight materials that maintain their rigidity during the spacecraft's orbital flight are essential for this application. The primary goal in designing the subsystem support structure was to meet the criteria for rigidity. During the launch phase, the structure will be tested to handle both static and dynamic stresses, with stiffness being the primary design criterion.

Specification of subsystem considered for Design:

- Sub system mass and Inertia.
- Mass : 1kg
- Ixx= 5384.81kg-mm^2, Iyy= 4661.9kg-mm^2, Izz= 1004.72kg-mm^2 C.G location=20mm above the subsystem interface.

ISSN: 1934--9955 www.ijise.net

Vol-15 Issue-01 Aug 2020

Figure 1: Representation of sub system

- First natural frequency > 70 Hz: To avoid coupling between bracket and rest of the spacecraft.
- Static analysis: 20g load taken in X, Y and Z directions independently.
- Buckling analysis: 20g load taken in X, Y and Z directions independently.

2. Problem Description

The main objective of the structural design is to achieve the minimum mass structure, which will satisfy the stiffness and strength requirements. Hence, optimum configuration, newer technological achievements have to be incorporated to attain minimum mass, which at the same time satisfy all the basic requirements.

Material Properties

Material used for subsystem support structure is AA-2024. Whose properties are given belo

Material	E (N\m^2)	ῦ	G (N\m^2)	Density(kg\m^3)
Aluminium	70E+9	0.30	26.8E+9	2800

E = Young’s Modulus of the Aluminum υ = Poison’s Ratio
G = shear Modulus of the AluminumSteps in Analysis

The following types of analysis are carried out:

1. Free Vibration Analysis
2. Static Analysis
3. Buckling analysis

1. Free vibration analysis (Eigenvalue analysis)

For a structural system with a total DOF of N, the stiffness matrix **K** and mass matrix **M** have a dimension of N ×N. In this technique, first solve the homogenous equation. The homogeneous equation is by considering the case of **F** = 0, therefore it is also called free vibration analysis, as the system is free of external forces. For a solid or structure that

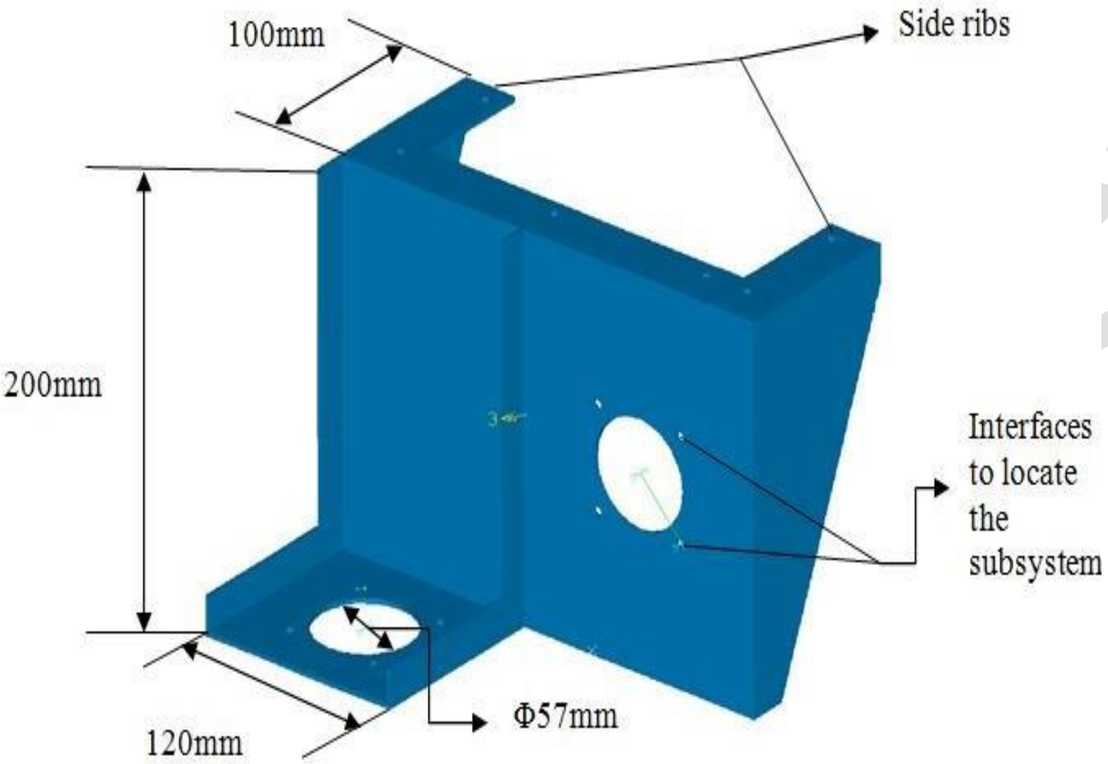

ndergoes a free vibration, the discretized system equation becomes.

$\mathbf{KD} + \mathbf{M}\ddot{\mathbf{D}} = 0$ (Eq.2.1)
This solution for the free vibration problem can be assumed as
$\mathbf{D} = \varphi \exp(i\omega t)$ (Eq.2.2)
Where **φ** is the amplitude of the nodal displacement, ω is the frequency of the free vibration, and t is the time.
By substituting Eq. (2.2) into Eq. (2.1), we obtain $[\mathbf{K} - \omega^2\mathbf{M}]\,\boldsymbol{\varphi} = 0$ (Eq.2.3)
or
$[\mathbf{K} - \lambda\mathbf{M}]\,\boldsymbol{\varphi} = 0$ (Eq.2.4)

where
$\lambda = \omega^2$ (Eq.2.5)

Equation (2.3) (or (2.4)) is called the eigenvalues equation. To have a non-zero solution for φ, the determinate of the matrix must vanish:

det [**K** − λ**M**] = |**K** − λ**M**| = 0 (Eq.2.6)

The expansion of the above equation will lead to a polynomial of λ of order N. This polynomial equation will have N roots, λ_1, λ_2. . . λ_N, called eigenvalues, which relate to the natural frequency of the system by Eq. (2.3).

3. Model Description

Subsystem support bracket (Option 1)Finite element model is shown in figure. Four noded quadrilateral shell elements having 5-degree of freedom per node is used to model the bracket. Mass of the subsystem is defined at center of gravity location. Lumped mass element each of 1kg is attached at the C.G location points to simulate the subsystem mass. This mass is equally distributed on the insert location of the subsystem by means of multipoint constraints (MPC).

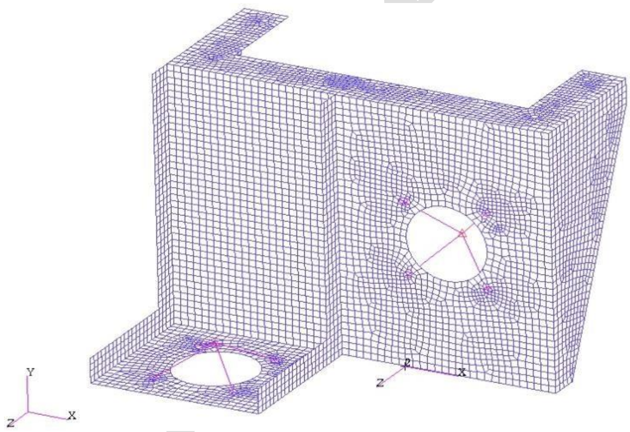

Figure 3: FE model

1. Boundary conditions:

For free vibration analysis, the boundary condition set consists of only the restraints set. The entire node at the insert location the bracket is restrained as Tx, Ty, Tz, Rx, Ry and Rz are fixed.

The size of bracket is 210mm x 270mm with height of 200mm. the top surface of the bracket consists of six interfaces used for connecting the bracket with deck. There are two cutouts dia.57mm, around which four interfaces each are provided to fix the subsystem.

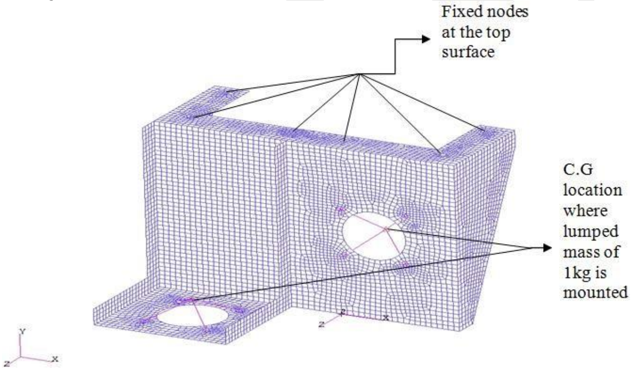

Figure 4: Boundary condition at top surface

2. Design parametric study:

The design parameter like thickness of the model was varied in order to select a suitable configuration. The variation of frequency with change in thickness for the model of configuration 1 is as shown below:Modified Subsystem Support Bracket (Option 2)

In the modified bracket one additional rib is provided at the mid with suitable interfaces. All other major dimensions are same as previous bracket.

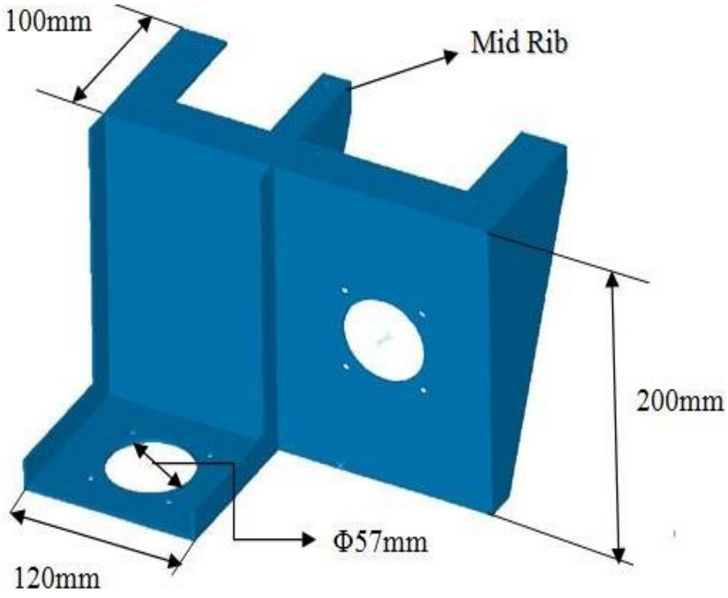
100mm
Mid Rib
200mm
Φ57mm
120mm

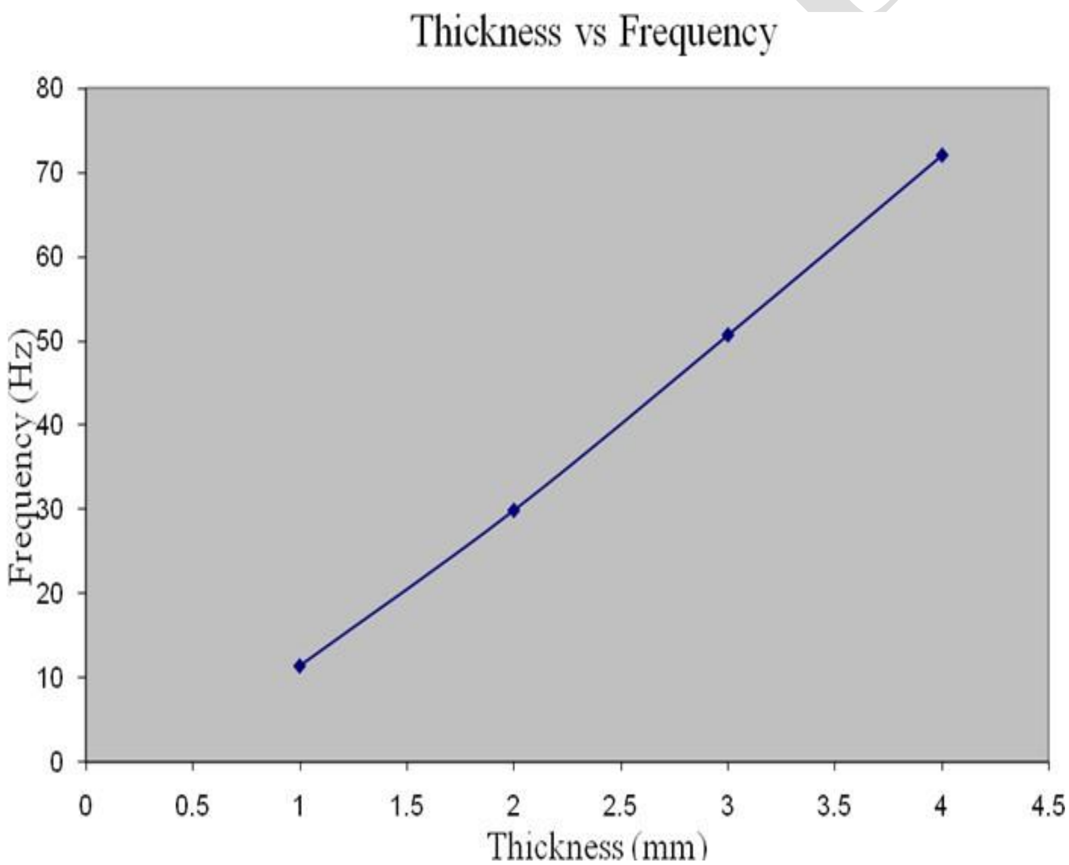
Thickness vs Frequency
Frequency (Hz)
Thickness (mm)
0
10
20
30
40
50
60
70
80
0.5
1
1.5
2
2.5
3
3.5
4
4.5

ISSN: 1934--9955 www.ijise.net

Vol-15 Issue-01 Aug 2020

Graph 1: Thickness vs. Frequency

1. FE model:**Figure 7:** 3D model

s it is observed from the graph 1 the change in the thickness of the bracket results in the change of the natural frequency of the structure. Since, the required frequency of 70 Hz is achieved with 4mm thicknesses that results in 1.2kg mass of the bracket. So, in order to minimize the mass for the desired frequency, design modification in the bracket is required. The mode shape of first and second natural frequencies with 2mm shell thickness is shown in fig below.

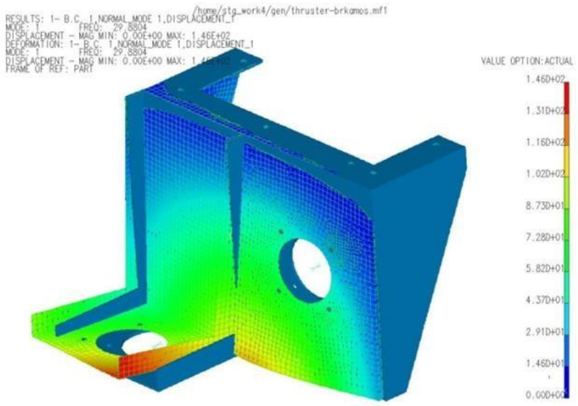

Figure 5: First mode shape (29.88Hz)

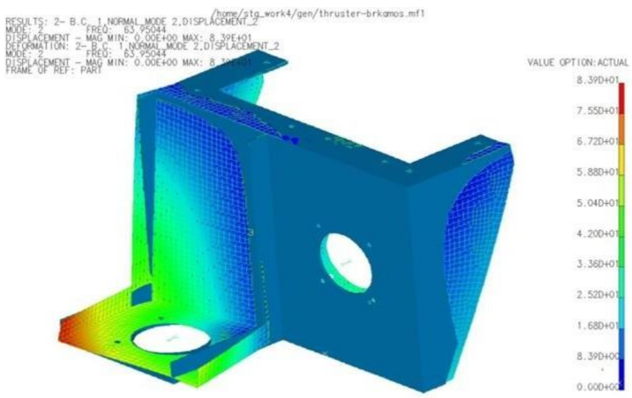

Figure 6: Second mode shape (63.95Hz)

Finite element model is shown in figure 8. Four noded quadrilateral shell elements having 5- degree of freedom per node is used to model the bracket. Mass of the subsystem is defined at C.G location. Lumped mass element each of 1kg is attached at the C.G location points to simulate the subsystem mass. This mass is equally distributed on the insert location of the subsystem by means of multipoint constraints (MPC).

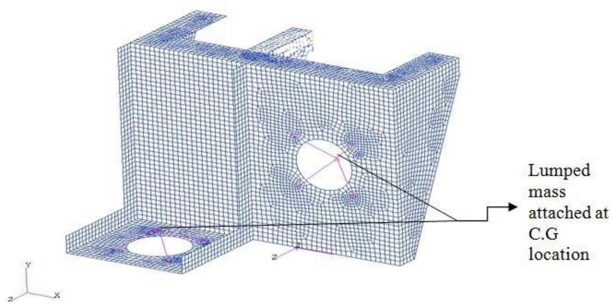

Figure 8: FE model

International journal of imaging science and engineering

ISSN: 1934--9955 www.ijise.net

Vol-15 Issue-01 Aug 2020

2. Boundary condition:

For free vibration analysis the boundary condition set consists of only the restraints set.

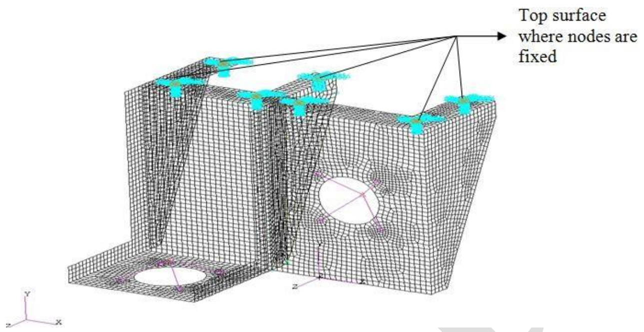

Figure 9: Boundary conditions at top surface

4. Design parametric Study:

The design parameter like thickness of the model was varied in order to select a suitable configuration. The variation of frequency with change in thickness for the designed thruster bracket is as shown below:

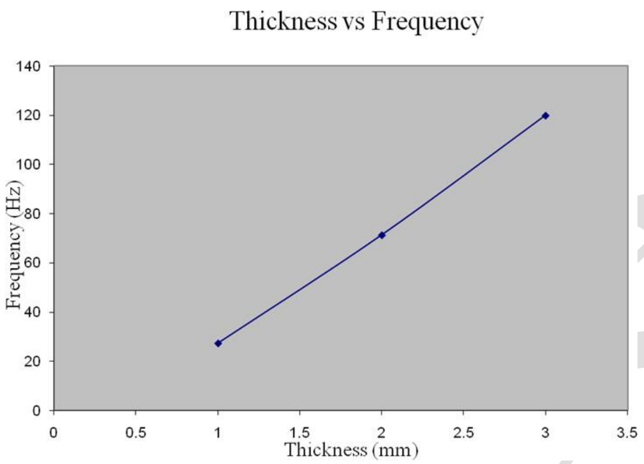

Graph 2: Thickness vs Frequency

As it is observed from the graph that change in the thickness results in the change of the natural frequency of the structure. The required frequency of 70 Hz is achieved with 2 mm thickness resulting mass of 0.697kg against 1.2kg as compared to the previous bracket. So, this model satisfies the stiffness criterion with minimum mass.

4. Static Analysis

In case of static structural analysis the loads are assumed to be applied slowly and the model is constrained to prevent rigid body motion. That is, Static equilibrium exists for the model.

<u>Model Description:</u>

Table 2: Check for interface forces

Load	Force in Kgf
20g-X direction	18.8
20g-Y direction	10.6
20g-Z direction	36.2

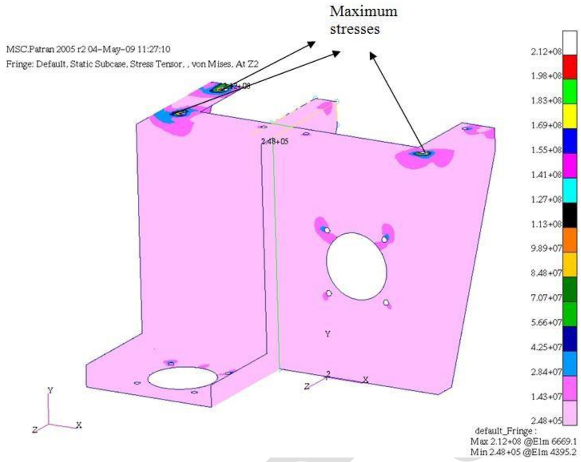

Figure 10: von mises stress for 20g load in X direction

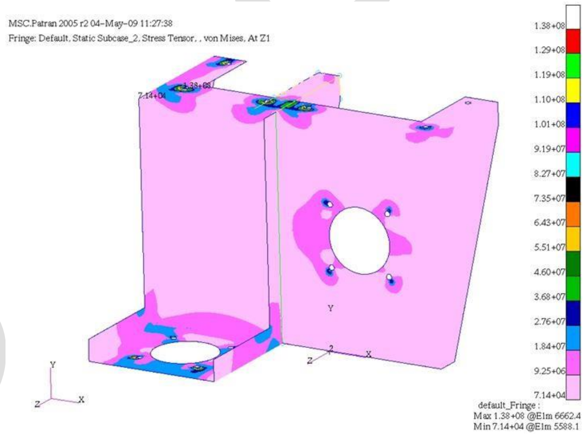

Figure 11: von mises stress for 20g load in Y direction

Linear static analysis was carried out to compute the response of structure for 20g load in X, Y and Z directions independently. I-DEAS linear static analysis was used for required purpose. The load entry was used to define the direction and magnitude of a gravity vector in Global Coordinate System.

5. Results and Discussion

Von mises stresses and interface forces are calculated for 20g load in X, Y, Z directions independently and results are given in table 4.1 and 4.2

Table 1: von mises stresses

International journal of imaging science and engineering

ISSN: 1934--9955 www.ijise.net

Vol-15 Issue-01 Aug 2020

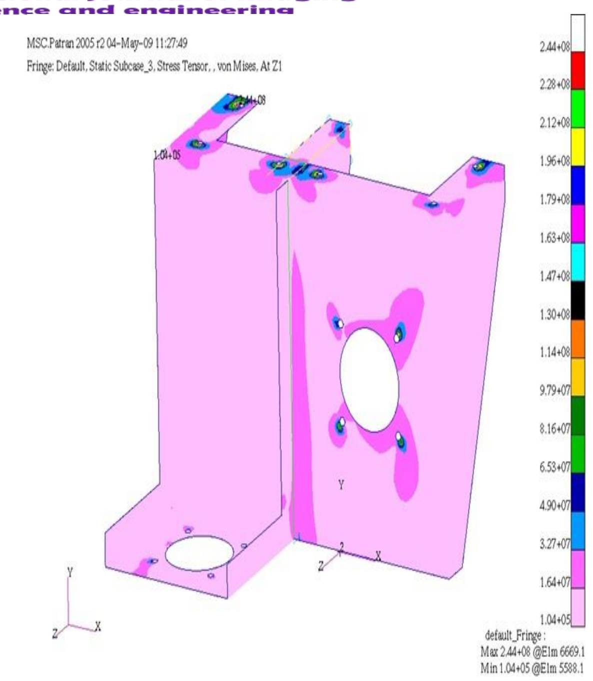

Figure 12: von mises stress for 20g load in Z direction

6. Buckling Analysis

In linear static analysis a structure is normally considered to be in a state of stable equilibriums the load is removed, the structure is assumed to return to its original position. However, under certain combination of loading, the structure may become unstable. When this loading is reached, the

load	Von mises stress (MPA)	Factor of safety (FOS)	Margin of safety (MOS=FOS-1)
20g-X direction	212	1.27	0.27
20g-Y direction	138	1.95	0.95
20g-z direction	212	1.27	0.27

structure continues to deflect without increase in magnitude of loading. In this case, the structure has actually buckled or has become unstable. Present study is performed for 20g forces in X, Y and Z direction.

Model Description:

Linear buckling analysis was carried out to compute the buckling failure of the structure for 20g force in X, Y and Z directions respectively. The fixed boundary condition was assumed at the connecting holes on the top surface of the bracket. I-DEAS Linear buckling analysis was used for the required purpose.

7. Results and Discussion

Buckling Load (20g)	Buckling Factor
Along X	23.48
Along Y	47.32
Along Z	11.22

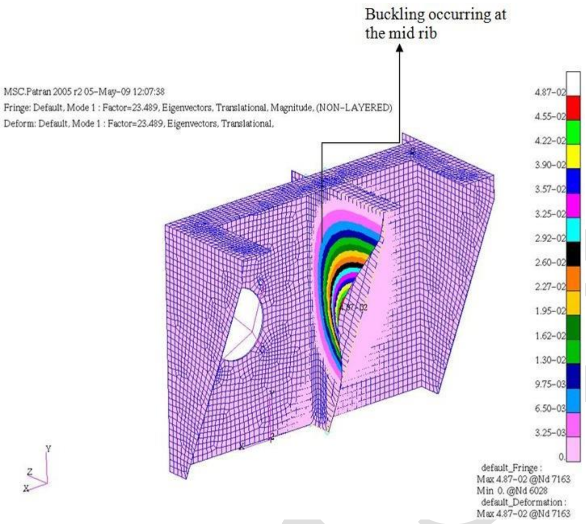

Figure 13: Buckling load for 20g in X direction

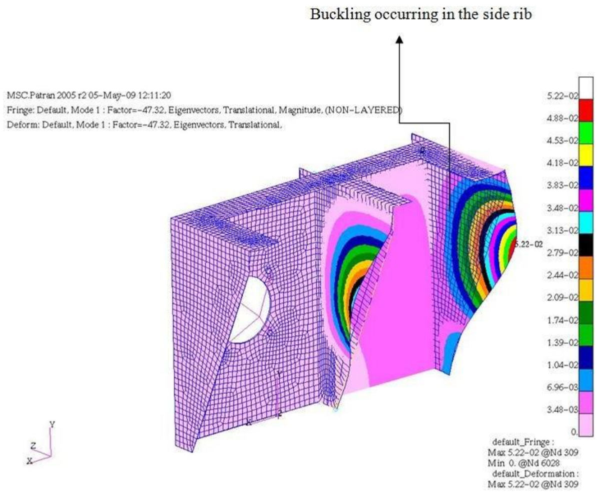

Figure 14: Buckling load of 20g in Y direction

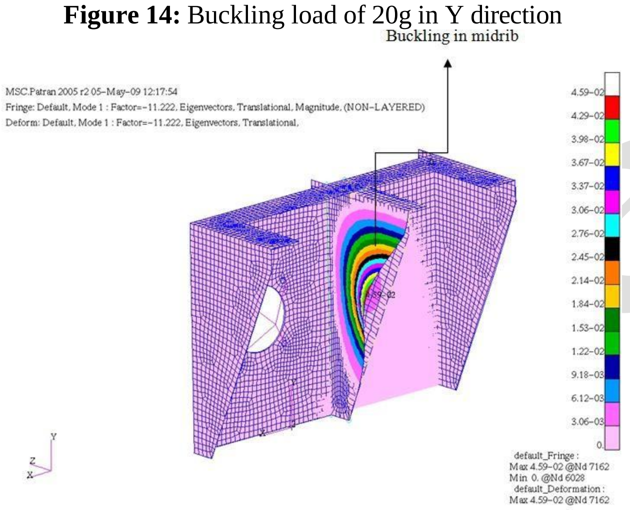

Figure 15: Buckling load of 20g in Z direction

8. Conclusion

The satellite subsystem support structure has been designed to support the deck of the satellite. The sensitivity analysis was carried out by varying design parameter like thickness. The configuration studied satisfies the stiffness requirement. The table below shows the comparison between Option 1 and Option 2.

SL.NO	Parameters	Option 1	Option 2
1	Thickness (mm)	4	2
2	1st mode Frequency (Hz)	71.99	71.29
3	2nd mode frequency (Hz)	148.8	84.48
4	Mass (kg)	1.2	0.697

International journal of imaging science and engineering

ISSN: 1934--9955 www.ijise.net

Vol-15 Issue-01 Aug 2020

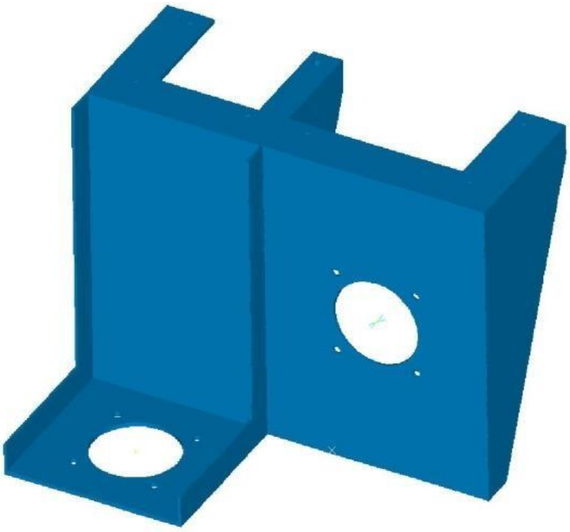

Figure 17: Option 2

References

[1] This is the 2004 Elmer A. Sperry Award.
The Rolls-Royce handbook [2].
Hybrid Propulsion-Electrical Installations, Rotterdam Mainport University of Applied Sciences—RMU, by A. Meerkerk, S. Zaalberg, N. Wit, W. V. Wijk, and H. Kievit.
[4] 2013 corporate brochure from Thrustmaster
Marine Propulsion by I. Martinez (4th edition).
[6] Definitions and words related to ships.
[7] In Science Direct, Ocean Engineering 31 (2004) 97-110, C.C. Liang and W.H. Cheng discuss the optimal control of thruster systems for dynamically positioned vessels.
The Adams Challenge for Diving Support Vessels: A Failure Modes and Effects Analysis [8] by D. Barton.
Referenced in the 2011 Journal of Polish CMAC, C. Dymarski and M. Zagórski presented a novel design for a pedestaled azimuth thruster for a small vessel's diesel-hydraulic propulsion system.
[10] Engineering Failure Analysis, October 2011, by M. Fonte, L. Reis, and M. Freitas, analyzed the failure of a gear wheel of a marine azimuth thruster.
In the Third International Symposium on Marine Propulsors smp'13, held in Launceston, Tasmania, Australia in May 2013, S. Go, Y. Ahn, J. Kim, and H. Seo conducted research on the powering performance of drillships in transit mode using azimuth thrusters.
[12] In the International Journal of Naval Architecture and Ocean Engineering (2013), T. Kim, S. Lim, H. Seok, and C. Kang presented a concurrent engineering solution for the design of ship and offshore bracket parts and fabrication process, with the reference number 5:376~39.
[13] A.V. Parab, Delft University of Technology, January 2015, Steering Torque Determination of Pulling Open Thrusters.
[14]Performance Characteristics of a Podded Propulsor During Dynamic Azimuthing, 8th Canadian Marine Hy., Islam M. F., Akinturk A., Liu P., and Veitch B.